EXPERIMENTAL STUDY ON THE DYNAMIC STABILITY OF THE IXV CONFIGURATION

Ali Gülhan, Josef Klevanski, Thomas Gawehn

Supersonic and Hypersonic Technology Department of the Institute of Aerodynamics and Flow Technology, German Aerospace Center (DLR), Linder Hoehe, 51147 Cologne, Germany,
Email: Ali.Guelhan@dlr, Josef.Klevanski@dlr.de, Thomas.Gawehn@dlr.de

ABSTRACT

Dynamic stability of the IXV configuration has been investigated using free oscillation measurement technique in the Trisonic Windtunnel (TMK). In the transonic Mach number range an escalating behavior of the pitching moment damping derivative has been observed, although the vehicle is statically stable. At Mach 0.8 the vehicle showed the most unstable behavior. The instability becomes weaker with increasing Mach number. At Mach number 1.1 the vehicle is only slightly instable. In the supersonic regime experimental data showed an excellent repeatability. All supersonic tests provided a negative pitching moment damping coefficient, i.e. dynamically stable vehicle behavior.

NOMENCLATURE

CFD	Computational Fluid Dynamics
$c_{m\alpha}$	Pitching moment stiffness coefficient
$c_{mq} + c_{m\dot{\alpha}}$	Pitching moment damping coefficient
c_y	Cross flexure stiffness
I_y	Moment of inertia
k_y	Cross flexure damping
L_{ref}	Reference Length
M	Moment
Ma	Mach number
p	Pressure
q	Dynamic pressure
Re_{Lref}	Reynolds number based on the reference length
S_{ref}	Reference area
α	Angle of attack [°]
δ	Damping decrement
ϕ	Sting incidence angle [°]
θ	Spring deflection angle [°]
ω	Oscillation frequency

1. INTRODUCTION AND OBJECTIVES

The aerodynamic behavior of the IXV configuration during its entry into the Earth atmosphere is a very important parameter for the success of the mission. The successful flight of IXV was carried out with deployed parachute at Mach numbers below 1.4. For possible future flights the vehicle performance has to be improved with respect to the maneuverability in transonic and subsonic speeds without parachute. In this flight regime the dynamic stability of IXV becomes a critical and important aspect.
The prediction of the dynamic stability using both experimental and CFD-tools is quite challenging. Special care is necessary for the preparation and performance of experimental and numerical activities. In the frame of the ESA TRP project 'Damping Derivatives Assessment for Hypersonic Re-entry Vehicles Exhibiting High Angle of Attack' dedicated experiments have been carried out in the Trisonic Windtunnel Cologne (TMK) of DLR in a Mach number range of 0.8 to 2 [1].

The objectives of the experimental study tests were:

- Measurement of the pitching moment damping coefficients of the IXV configuration
- Measurement of the pitching moment stiffness coefficients

2. EXPERIMENTAL TOOLS

2.1. Trisonic Windtunnel Cologne (TMK)

TMK is a trisonic blow down windtunnel with a cross section of 0.6 m x 0.6 m [2]. It is equipped with a flexible nozzle. Standard Mach number range is 1.25<Ma<4.5. Mach numbers up to 5.7 can be reached by means of a storage heater and an ejector. For Mach numbers of 0.5<Ma<1.2 a transonic test section with perforated walls is available. The maximum running time depending on Mach and Reynolds numbers is up to 60 seconds. *Figure 1* and *Figure 2* show a picture and the performance map of the facility, successively.
The Mach number and Reynolds number range of TMK is supplemented by the neighboring hypersonic facility H2K in which the same models can be tested. The Mach-Reynolds map of the facility for a model length of 125 mm is shown in comparison with the flight trajectory of IXV (*Figure 2*). The operation of TMK without ejector allows a very close match to flight conditions in a Mach number range between 0.8 and 2.

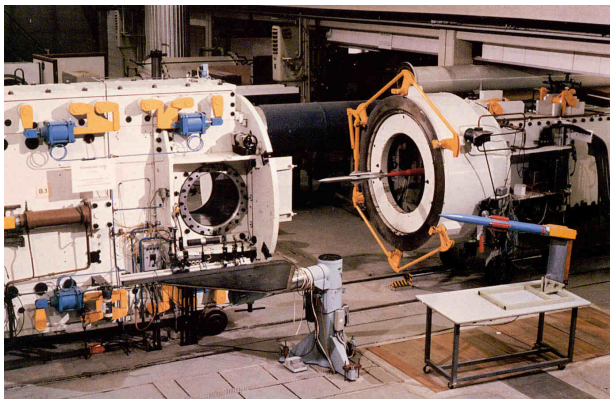

Figure 1. Trisonic Windtunnel TMK

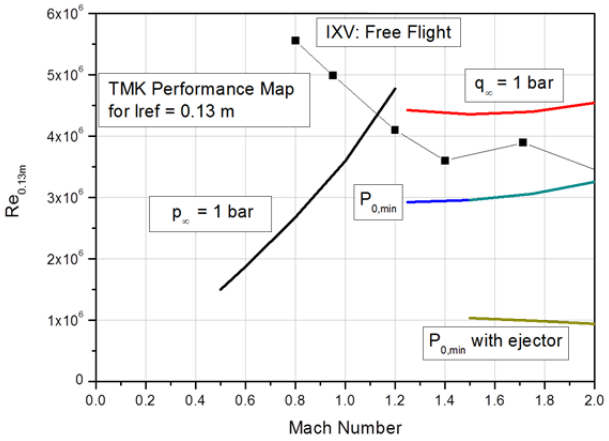

Figure 2. Performance map of TMK in comparison to the IXV flight trajectory.

2.2. Windtunnel Model

The model scale is 1:35.2, i.e. the model reference length is 125 mm (without flaps) and the reference surface is S_{ref} = 0.0058594 m^2. The Model Reference Center (MRC) is defined as 58% of ref. length along X axis, -2.5% along Z axis, 0 along Y axis [3].

Moment of inertia and cross flexure stiffness were chosen to get the same reduced frequencies in the windtunnel tests than expected for flight conditions. For dynamic tests, the model is designed in a way that the center of gravity (CoG) and the center of rotation (CoR) are as close as possible to the model reference center (MRC) defined in [3]. Therefore special trim weights of a high density material were integrated in the front and the back of the model.

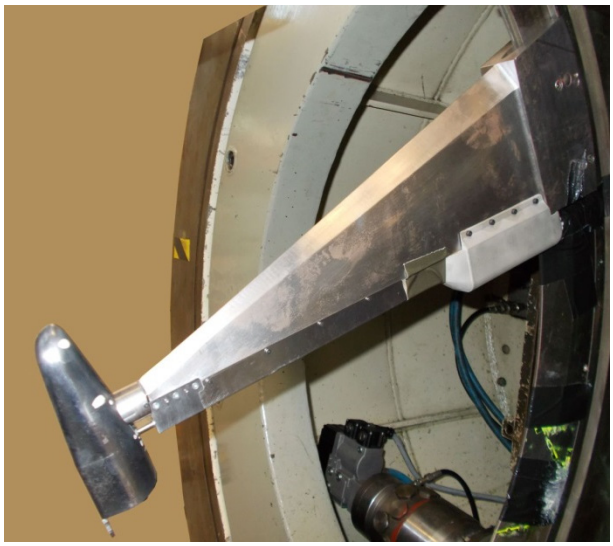

Figure 3. IXV model in TMK.

Based on the results of the static tests the flap deflection angle of 0° was the baseline of dynamic tests. But the model design allowed also testing at ±5° flap deflection. Therefore, with respect to the trim conditions derived from static tests, an angle of attack range of 37°<α<67° and axial force of -140 N, normal force of -850 N and side force of less than ±10 N were set as requirements on the model design.
The windtunnel model in TMK is shown in *Figure 3*, the main model parameters are listed in *Table 1*.

Table 1. Main test model characteristics

Characteristic	Value
Scale	1:35.2
Reference Length L_{ref} (without flaps)	0.125 m
Reference Area S_{ref}	0.0058594 m²
Mass m	1.478 kg
Coordinate $X_{CoG} = X_{COR} = X_{MRC}$	$0.58 \cdot L_{ref}$ = $72.5 \cdot 10^{-3}$ m
Coordinate $Y_{CoG} = Y_{COR} = Y_{MRC}$	$0.00 \cdot L_{ref}$ = 0.00 m
Coordinate $Z_{CoG} = Z_{COR} = Z_{MRC}$	$-0.025 \cdot L_{ref}$ = $-3.125 \cdot 10^{-3}$ m

2.3. Free oscillation measurement technique

The key element of the experimental set-up is the elastic cross-flexure (*Figure 4*). It is designed to provide the necessary motion around the CoR, which has to be as close as possible to CoG. The stiffness of the cross-flexure was defined by considering the duplication requirement with respect to the reduced frequency in addition to Mach and Reynolds number duplication. The cross flexure should also allow to get about 20 oscillation cycles for 3 different releases during one run.

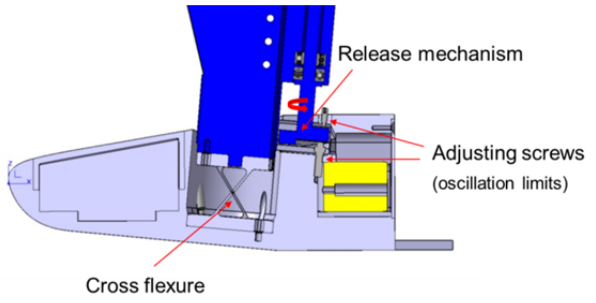

Figure 4. Cross section view of the model.

Cross flexures of different stiffness (c_y = 1, 4 and 6 Nm) were designed and manufactured to avoid robustness problems and to assess reduced frequency parameter effects. The model with the integrated cross-flexure is mounted to the sting, which contains the electric stimulation / release mechanism. The initial amplitude of the oscillation is defined by an adjusting screw. The same system allows also catching of the model and stopping the oscillation. The control of the model releasing and catching is provided by special software in LabView-version.

In order to avoid any damages to the cross flexure, the model deflection is limited to ±3°. Depending on the test parameters the initial deflection amplitude is set to ±2…3°. The cross-flexure is equipped with two special strain gauges (DMS). The strain gauges are connected to Wheatstone bridge circuits. The measured DMS-voltage signals correspond to the deflection angle θ of the cross-flexure. These analogue signals are transformed by an analog-to-digital converter and recorded by LabView application with a sampling rate of 1000 Hz.
The sting is made out of a steel 1.0553. It is designed to minimize the interaction with the wake in a wide range of high angle of attack (40°…75°).

2.4. Cross Flexure Calibration

The main objective of the calibration is the determination of the cross-flexure characteristics i.e. stiffness and damping. The cross-flexure calibration also provides the coefficient of the deflection angle calculation from the electrical signal

The cross-flexure stiffness and the electric sensibility of the DMS for the measurement of deflection angle is determined by the static calibration performed with the special static calibration device, which is fixed to the movable support. The mechanical moment is produced by placing of the etalon i.e. device with exactly defined mass (213.6 g) on several pre-defined positions on the horizontal bar of the calibration device. The resulted deflection of the calibration device due to the cross-flexure deformation is compensated by rotation of the support. The orientation of the horizontal bar was restored and the compensating angle of the support equals exactly the cross-flexure deformation.
The cross flexure has two strain gauges. Their linear regression was measured during calibration experiments. *Figure 5* shows the signals of both strain gauges DMS1 and DMS2 of the cross-flexure.

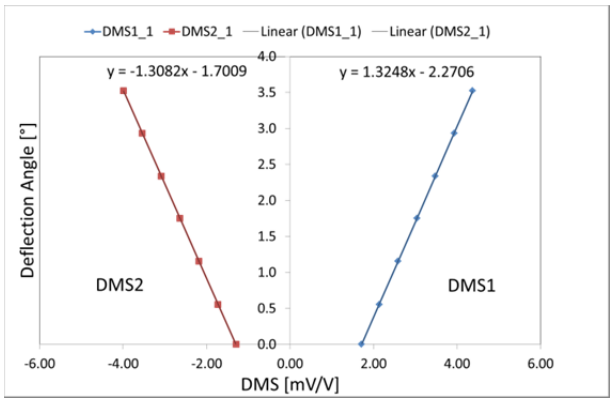

Figure 5. Measured relation between deflection angle and DMS signal for both strain gauges.

The values of the stiffness coefficient c_y were estimated from the dependencies $M = f(\theta)$ measured via calibration device for several balanced disk combinations providing the calibrated axial force. The resulted stiffness dependency on the axial force, i.e. $c_y = f(F_{ax})$ is given in *Figure 6*. The estimated stiffness for cross-flexure 1 is $c_y = -(4.025 + 0.0033 \cdot F_{ax})$ Nm/rad.

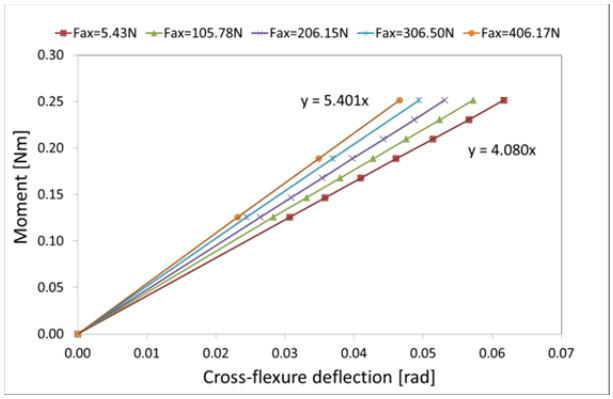

Figure 6. Measured mechanical stiffness in dependency of the axial force.

The main objectives of the dynamic calibration are to estimate the moment of inertia of the windtunnel model I_y and the damping characteristic of the flexure without flow $k_y(\omega)$. For this task a specially designed dynamic calibration device was used. It has special catches for the etalon disks, with the known geometry and inertia characteristics. This device is fixed to the cross-flexure and both are mounted to the sting which contains the release mechanism. The free oscillations are initiated

via this release mechanism. The cross-flexure damping depends on the oscillation frequency. Therefore the disc combinations are specially defined to provide the necessary reference frequencies for the whole range of the designed frequency range.

The results of the dynamic calibration tests were processed with the special identification routine **R2LIN** from the **IMSL**-library. The frequency ω and the corresponding damping δ_{va} are estimated [4].

The moment of inertia was estimated from the dynamic calibration tests of the cross-flexure 1. The results are presented in *Figure 7*. The linear regression was used for the dependency $I_{y\ Disc\ Comb} = f(1/\omega^2)$. The regression coefficients 4.075 correlates well with the value coming from the static calibration of the cross-flexure (c_y = 4.05). The damping decrement δ on frequency ω is also approximated linearly as shown in *Figure 8*.

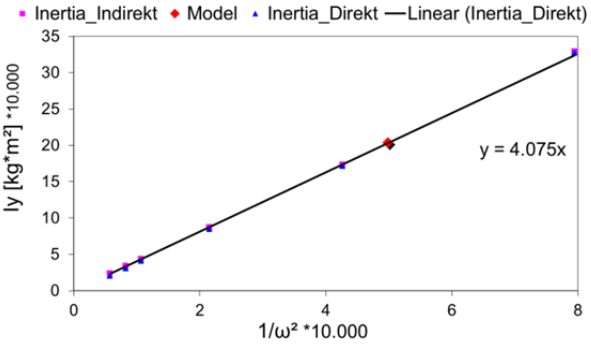

Figure 7. Measured moment of inertia.

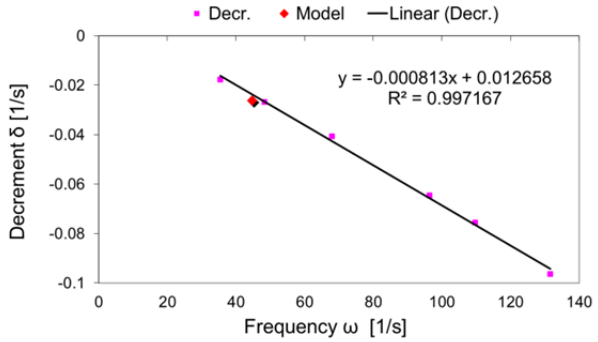

Figure 8. Measured mechanical damping.

3. EXPERIMENTS

3.1. Flow parameters

For the tests the standard operation mode of TMK (without ejector) was used. The flow parameters listed below are computed from the measured reservoir pressure, total temperature and the known nozzle geometry, i.e. Mach number.

Table 2. Flow parameters.

Ma	P_0 [bar]	T_0 [K]	q_∞ [Pa]	Re_{LRef}	RFP
0.80	1.53	290	44966.3	2.67E+06	0.041
0.85	1.62	290	51085.3	2.91E+06	0.039
0.90	1.71	290	57326.8	3.15E+06	0.037
0.95	1.80	290	63619.0	3.38E+06	0.036
1.10	2.22	290	88066.5	4.32E+06	0.035
1.15	2.70	290	109936.4	5.28E+06	0.031
1.30	1.93	290	82403.5	3.77E+06	0.028
1.40	2.07	290	89245.7	4.00E+06	0.028
1.45	2.12	290	91332.5	4.06E+06	0.027
1.50	2.13	290	91384.4	4.04E+06	0.020
1.60	2.14	290	90223.7	3.96E+06	0.020
1.70	2.29	290	93854.9	4.11E+06	0.020
1.80	2.35	290	92760.0	4.07E+06	0.200
2.00	2.70	290	96620.2	4.32E+06	0.018

3.2. Test procedure

Before each dynamic test the sting angle was adjusted based on the trim angle data gained during static tests. It has been noticed that the trim angle of dynamic tests was slightly different. The possible explanation is the difference in the geometry of the model support arm, which was slender for dynamic tests. The pre-setting of the initial defection angle had to be carried out with care.

Before each run a dry run without flow was performed to check the mechanical stiffness and damping behavior of the cross flexure. This step was at the same time a check of the measurement techniques and data acquisition.

3.3. Transonic tests

First tests were carried out using cross-flexure 1 with 0° flap angle. All transonic tests were performed on the model with smooth surface. The test matrix and the estimated pitching moment damping coefficients $c_{mq} + c_{m\dot{\alpha}}$ and pitching moment stiffness coefficients $c_{m\alpha}$ are given in *Table 3*.

Table 3. Transonic test matrix.

Run no.	Ma	Sting angle [°]	Initial deflection angle [°]	loops	Duration [s]	Tripping	$c_{mq} + c_{m\dot{\alpha}}$ [-]	$c_{m\alpha}$ [1/°]
18	0.8	63.6	0	3	3	no	1.51767	-0.00557
19	0.8	62.83	0	7	1	no	1.38143	-0.00514
21	0.95	59.8	0	3	3	no	0.03054	-0.00298
22	0.95	59.8	2.98	3	3	no	0.15350	-0.00345
23	1.1	57.9	2.98	1	1	no	-0.12570	-0.00305
24	1.1	57.9	2.98	3	3	no	0.00337	-0.00310
26	0.9	61.7	2.98	3	3	no	0.08327	-0.00361
30	0.85	62.5	0	1	1	no	0.67030	-0.00406
31	0.9	61.7	~0.5	1	1	no	0.60670	-0.00361
32	0.9	61.7	~0.5	3	1	no	0.09600	-0.00353
33	0.9	62.2	1	3	1	no	0.30389	-0.00342
34	1.1	57.9	1	3	3	no	0.18387	-0.00341
46	1.1	57.9	3	1	2	no	0.01717	-0.00317
48	1.135	58.28	3	1	2	no	-0.17470	-0.00215

During tests it has been noticed that in transonic flow regime the data is extremely sensitive to any changes in the flow field. Therefore some tests have been repeated

to gather sufficient data for the data reduction with a better confidence level. It was noticed that the vehicle is dynamically unstable at Ma=0.8. Because of strong escalation of the pitch oscillation the deflection angle reaches the limit angle of about 4°, defined by the available space of the model rear part, very fast. But at least 3-4 cycles allowed a reasonable curve fitting and determination of the pitch damping coefficients. As shown in *Figure 9* the software, which identifies the useful cycle range for the curve fitting, rejects some cycles of this run. The same post-processing analysis was also applied to a former dynamic stability study on the Exomars capsule [5].

All runs at Ma=0.95 indicated a slight unstable pitch damping behavior of the vehicle (*Figure 10*). Further increase in the Mach number to Ma=1.1 leads to almost indifferent behavior. Tests at Ma=0.9 provided partially remarkably different results in terms of the pitching moment damping coefficient. Therefore at this Mach number several repeatability tests have been carried out. In average the data show a slight escalating behavior. Since the difference in the pitching moment damping coefficients at Mach numbers 0.8 and 0.9 was significant (although in both cases an escalating oscillation was measured), an additional run was carried out at Ma=0.85. A clear escalating pitch oscillation has been measured.
The estimated pitching moment stiffness coefficients $C_{m\alpha}$ are shown in *Figure 11*. The vehicle is statically stable in the complete transonic flight regime.

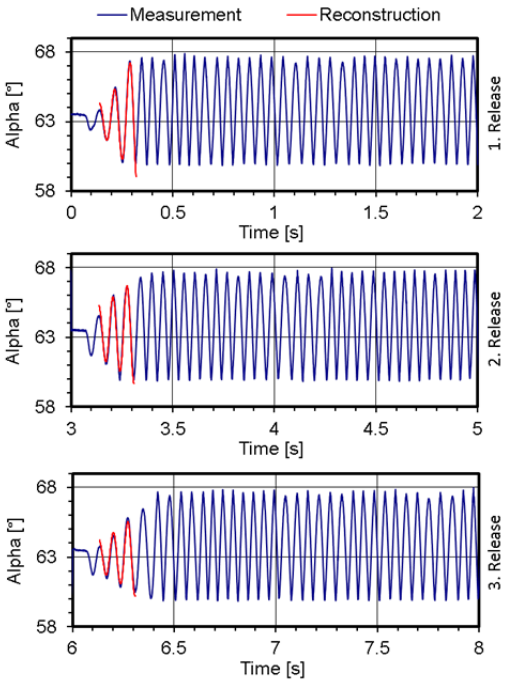

Figure 9. Oscillation cycles at Mach 0.8.

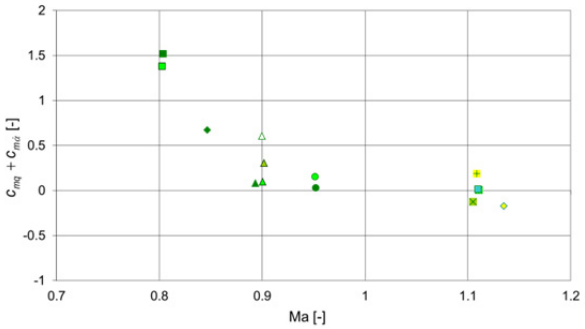

Figure 10. Measured pitching moment damping coefficients at transonic speeds.

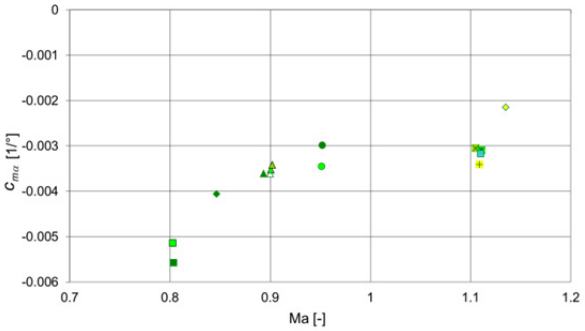

Figure 11. Measured pitching moment stiffness coefficients at transonic speeds.

3.4. Supersonic tests

After completion of transonic tests and careful analysis of the data the TMK test configuration has been changed to the supersonic one. As shown in *Table 4* tests have been carried out in a Mach number range of Ma = 1.3 – 2.0. Supersonic tests were started with the flap angle of 0°, in order to compare the data directly to the transonic test cases. Further runs have been performed on a rough surface at Mach numbers of 1.5 and 1.4 to investigate the influence of the surface roughness on the dynamic stability. The test matrix and determined data of $c_{mq}+c_{m\dot{\alpha}}$ and $c_{m\alpha}$ are given in *Table 4*.

Table 4. Supersonic test matrix.

Run no.	Ma	Sting angle [°]	Initial deflection angle [°]	loops	Duration [s]	Tripping	$c_{mq}+c_{m\dot{\alpha}}$ [-]	$c_{m\alpha}$ [1/°]
60	2.0	40.05	2.7	3	4	no	-0.28317	-0.00127
61	1.8	40.05	2.6	3	4	no	-0.27287	-0.00133
62	1.8	38.5	2.6	3	4	no	-0.26570	-0.00164
65	1.5	38	2.6	1	2	no	-0.20270	-0.00141
67	1.5	38	2.6	3	2	no	-0.22617	-0.00142
76	1.3	56	2.6	1	2	no	-0.16260	-0.00267
77	1.3	56	2.6	3	4	no	-0.04101	-0.00265
80	1.4	56	1	3	4	no	0.23660	-0.00263
81	1.4	56	1	3	3	no	0.09144	-0.00273
82	1.4	56	1	3	3	no	0.14500	-0.00271
83	1.3	56	1	3	3	no	-0.00443	-0.00252
84	1.3	56	1	3	3	no	-0.05940	-0.00254
86	1.3	51	1	3	3	no	0.07324	-0.00277
99	1.7	37	2.6	3	3	no	-0.20853	-0.00195
100	1.6	37	2.6	3	3	no	-0.24190	-0.00191
101	1.5	38	2.6	3	3	yes	-0.19730	-0.00185
102	1.4	56	2.6	3	3	yes	-0.07092	-0.00273

As shown in *Figure 12* at the Mach number 2 the pitch oscillation has a strong damping behavior, i.e. the IXV configuration is dynamically stable. The repeatability of the data between three cycles is excellent.

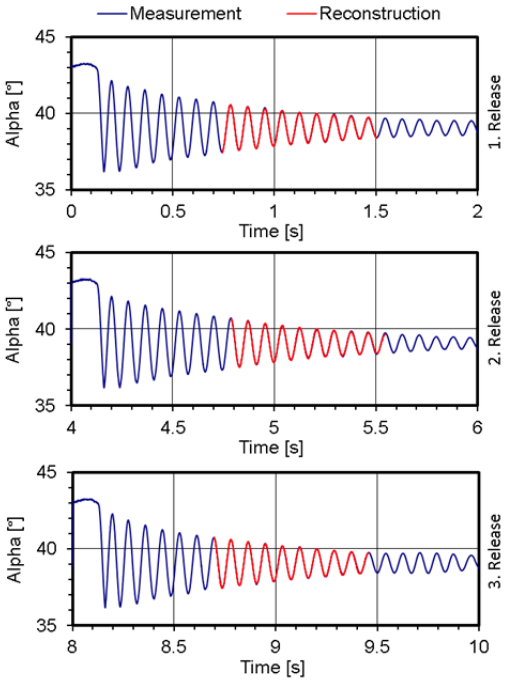

Figure 12. Oscillation cycles at Mach 2.0.

Determined values of the pitching moment damping coefficients $c_{mq} + c_{m\dot{\alpha}}$ are shown in *Figure 13*. The situation for the Mach number 1.5 is similar. Tests at Ma=1.4 did not show a repeatable stable behavior. Therefore four runs were carried out to collect sufficient data at this Mach number. The vehicle tends to be dynamically unstable although statically stable (*Figure 14*). At Ma=1.3 the vehicle is dynamically almost stabile or indifferent. Further tests at Mach numbers 1.6 and 1.7 allowed to confirm the dynamic stability of the IXV configuration at Mach numbers above Ma=1.4 clearly.

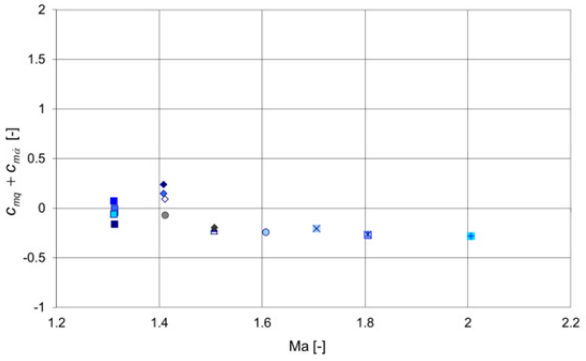

Figure 13. Measured pitching moment damping coefficients at supersonic speeds.

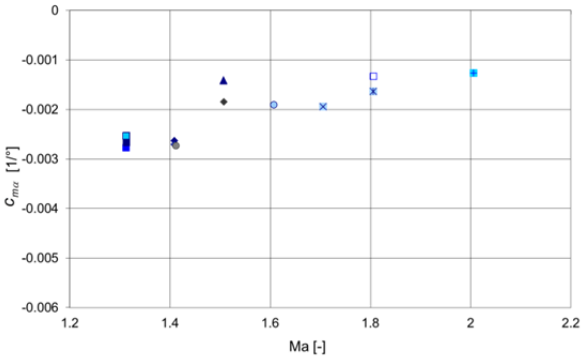

Figure 14. Measured pitching moment stiffness coefficients at supersonic speeds.

Further tests were performed with a flap deflection angle of -5° that reduces the trim angle of the IXV vehicle. The expected increase in dynamic stability for Mach numbers above 1.5 is confirmed.

4. ACKNOWLEDGEMENTS

The authors express their special acknowledgement to the European Space Agency (ESA) for the financial and technical support of this project.

5. CONCLUDING REMARKS

The main results of the experimental study on the dynamic stability of the IXV configuration (*Figure 15*) can be summarized as follows:

- In the transonic Mach number range (Ma = 0.8 - 1.1) with 0° flap deflection an escalating behavior of the pitching moment damping derivative has been observed, although the vehicle is statically stable. At Mach 0.8 the vehicle showed the most unstable behavior. The instability becomes weaker with increasing Mach number. At Mach number 1.1 the vehicle is only slightly instable. The repeatability of transonic tests was not satisfactory. Therefore more tests were carried out to have a better statistical evaluation of the data.

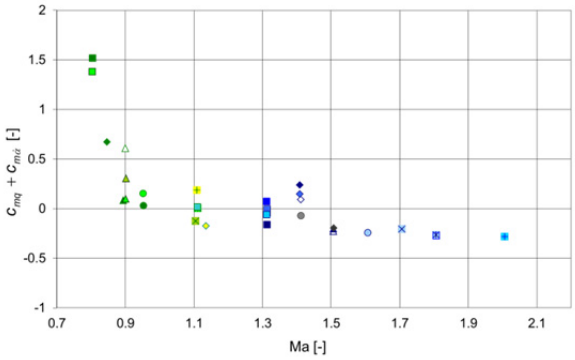

Figure 15. Measured pitching moment damping coefficients of IXV.

- In the supersonic regime experimental data showed an excellent repeatability in the Mach number range of Ma = 1.5 - 2). All tests provided a negative pitching moment damping derivative, i.e. dynamically stable vehicle behavior.
- The IXV configuration showed around Ma=1.4 an unexpected higher dynamic instability compared to lower and higher Mach numbers. In order to understand this phenomena several repetition tests at Mach 1.4 and additional tests at Mach numbers 1.45 and 1.3 were carried out. These tests confirmed the slight increase of the dynamic instability around Mach number 1.4.
- Tests with a rough surface did not show any difference in the pitching moment damping or stiffness coefficients at the Mach numbers 1.4 and 1.5.
- The results indicate an influence of the sting on measured data at Mach numbers below 40°. Since the model support arm was designed for high angle configurations, the data at high trim angles are less influenced by the sting.

Finally an Aerodynamic Data Base (AEDB) has been created using the experimental and numerical data of the DERIVAS study [6,7]. *Figure 16* shows the AEDB of DERIVAS derived from the uncertainty estimation of experiments and numerical simulation of the configuration with sting.

6. REFERENCES

1. Statement of Work, Damping Derivatives Assessment for Hypersonic Re-entry Vehicles Exhibiting High Angle of Attack, ESA Directorate of Technical and Quality Management TEC-MPA/2010/JS, Issue 1, Revision 1, 11. September 2010.
2. Esch, H.; Die 0.6-mx0.6-m-Trisonische Meßstrecke (TMK) der DFVLR in Köln-Porz, DFVLR-Mitt. 86-21, März, 1986.
3. DERIVAS model design and manufacturing report. TN4000, Issue 1, Rev. 0, 30.05.2013.
4. DERIVAS report on instrumentation and calibration of experimental setup. TN5000, Issue 1, Rev. 0, 30.08.2013.
5. A. Gülhan, J. Klevanski, S. Willems; Experimental Study of the Dynamic Stability of the Exomars Capsule, 7th European Symposium on Aerothermodynamics of Space Vehicles, 2011.
6. DERIVAS damping derivatives tests on the IXV Re-entry vehicle in the DLR trisonic windtunnel TMK. TN6000, Issue 1, Rev. 0, 12.12.2013.
7. DERIVAS report on numerical computation of damping derivatives. TN7100/TN7200, Issue 1, Rev. 0, 12.12.2013.

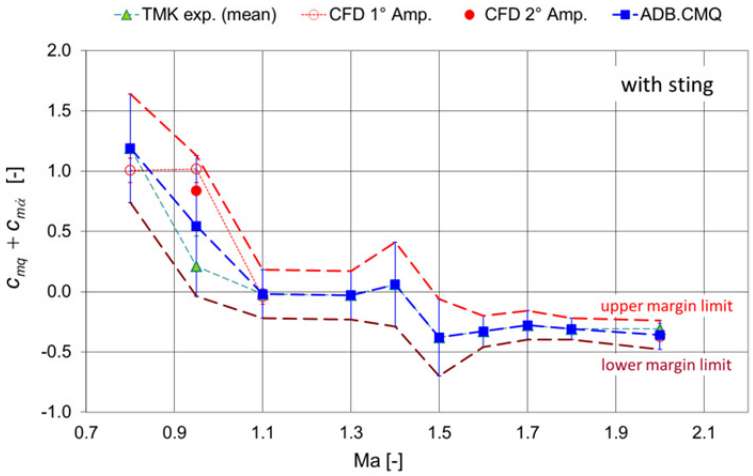

Figure 16. DERIVAS AEDB concerning the dynamic stability of the IXV configuration.